LUND UNIVERSITY

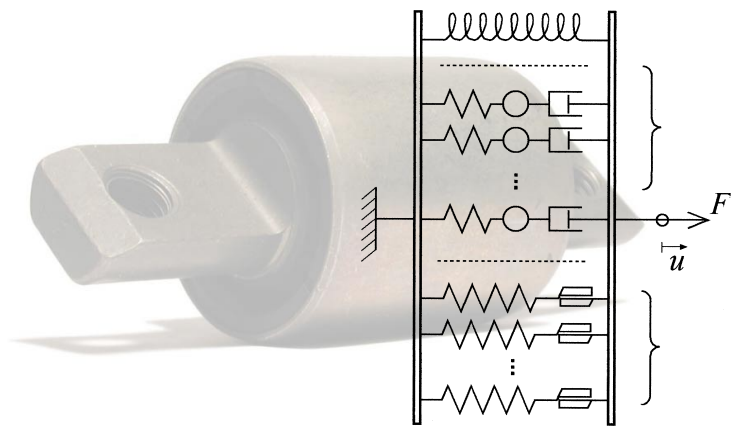

HYDROBUSHING MODEL FOR MULTI-BODY SIMULATIONS

MALIN SVENSSON and MARIE HÅKANSSON

Structural Mechanics

Master's Dissertation

Structural Mechanics

ISRN LUTVDG/TVSM--04/5124--SE (1-53)
ISSN 0281-6679

HYDROBUSHING MODEL FOR MULTI-BODY SIMULATIONS

Master's Dissertation by

MALIN SVENSSON and MARIE HÅKANSSON

Supervisors:

Per-Erik Austrell, Div. of Structural Mechanics

Anders Wirje, Volvo Car Corporation

Printed by KFS I Lund AB, Lund, Sweden, April 2004.

For information, address:
Division of Structural Mechanics, LTH, Lund University, Box 118, SE-221 00 Lund, Sweden.
Homepage: http://www.byggmek.lth.se

Preface

The work presented in this Master's thesis was carried out at the Division of Structural Mechanics, Lund University, Sweden in cooperation with the Strength and Durability Centre of Volvo Car Corporation during September 2003 - April 2004.

We would like to express our gratitude to our supervisor, Ph.D. Per-Erik Austrell at the Division of Structural Mechanics, for his guidance during this work. We would also like to thank our supervisor M.Sc. Anders Wirje at Volvo Car Corporation for supporting us with thoughts and ideas. A special thanks to Graphics Technician Bo Zadig at the Division of Structural Mechanics for creating some of the pictures used in this report.

Lund, April 2004

Marie Håkansson and Malin Svensson

Abstract

The purpose of this Master's thesis is to establish a methodology for hydrobushing modelling and parameter identification. The studied hydrobushing is used as a connector element between suspension components in Volvo S60, S80, V70, and XC70. The hydrobushing has coupled amplitude and frequency dependence. At Volvo Cars there is a need for a component model, which fully captures this property.

Experimental tests have been performed at the Materials Centre laboratory at Volvo Cars, and this data is used to establish the hydrobushing model. The model consists of one non-linear spring, several fluid elements and elasto-plastic elements coupled in parallel. An automatic fitting procedure finds the set of model parameter values that gives the best fit of the calculated response to the experimental data. The fitting procedure is based on hysteresis fitting, where each calculated data point in a hysteresis loop is compared to the corresponding experimental one and the deviation is minimized.

In the validation process it turns out that the hydrobushing model, however, is not able to completely capture the coupled amplitude and frequency dependence of the component. The model is seen to underestimate the damping for dynamic loading at small amplitudes (≤ 0.2 mm). Dynamic loading at amplitudes larger than 0.2 mm, as well as static and quasi-static loading, are represented in a satisfying way.

Contents

Chapter 1

Introduction

1.1 Background and objective

Rubber components such as rubber bushings, hydrobushings, hydraulic engine mounts, and jounce bumpers constitute a vital element in vehicle suspension systems since they often are crucial for the dynamic behaviour. The rubber components are used as connector elements in the suspension system and as an interface between the chassis and the body structure. Dynamic simulations of systems including rubber elements are complex, due to the fact that the dynamic characteristics depend on several variables, e.g. amplitude, frequency, preload, and temperature.

A hydrobushing is a combined elastomeric and hydraulic system, which consists of natural rubber and cavities partly filled with a fluid (glycol). The fluid can flow between chambers through channels. By using a hydrobushing, stiffness and damping properties not possible to achieve with conventional rubber bushings can be provided. The dynamic behaviour is characterized by very high damping at a specific frequency, where the fluid comes into resonance. Hydrobushings are useful for NVH (Noise, Vibration, and Harshness) control.

Multi-body simulations of full vehicles and subsystems are carried out in the automotive industry to analyse durability, handling, and ride comfort. The Multi-Body-System (MBS) code ADAMS is used at Volvo Cars. The component models of rubber elements have proven to be critical for the quality of the simulations. As considering bushing models at Volvo Cars, there is a need to be able to fully capture the coupled frequency and amplitude dependence of a hydrobushing.

The main objective of this thesis is to establish a methodology for hydrobushing modelling and parameter identification.

1.2 Overview

This Master's thesis is a cooperation between Volvo Car Corporation and the Division of Structural Mechanics, Lund Institute of Technology, Lund University. The major activities have been to:

- Propose a hydrobushing model, which models both rubber and fluid.
- Develop an automatic fitting procedure that fits the model parameters to the experimental results.
- Validate the hydrobushing model by comparison with component testing.

The modelling and identification is performed in MATLAB. The model can be implemented into commercial MBS codes like ADAMS.

1.3 Outline

Chapter 2: Hydrobushing properties This chapter is a presentation of the analysed component. The design and the dynamic characteristics of the hydrobushing are described.

Chapter 3: Laboratory experiments A description of the test method is given in this chapter, although the focus is on the test results. The static, quasi-static, and steady state harmonic dynamic characteristics of the hydrobushing are analyzed and hysteresis loops are studied in detail.

Chapter 4: Hydrobushing modelling The hydrobushing model is presented and the equations that build up the model are derived/presented.

Chapter 5: Fitting procedure This chapter describes the development and the function of the automatic parameter fitting procedure.

Chapter 6: Validation In this chapter the hydrobushing model is compared to experimental results. This is performed by comparison of hysteresis loops.

Chapter 7: Summary and conclusions The work is summarized and conclusions from the validation are drawn. Ideas on improvements of the hydrobushing model are also discussed.

Chapter 2

Hydrobushing properties

A hydrobushing is a component used in vehicle systems to control NVH (Noise, Vibration, and Harshness) and ride comfort. The studied hydrobushing is used as a connector element between the suspension components in Volvo S60, S80, V70, and XC70. Figure 2.1(a) shows the position of the hydrobushing.

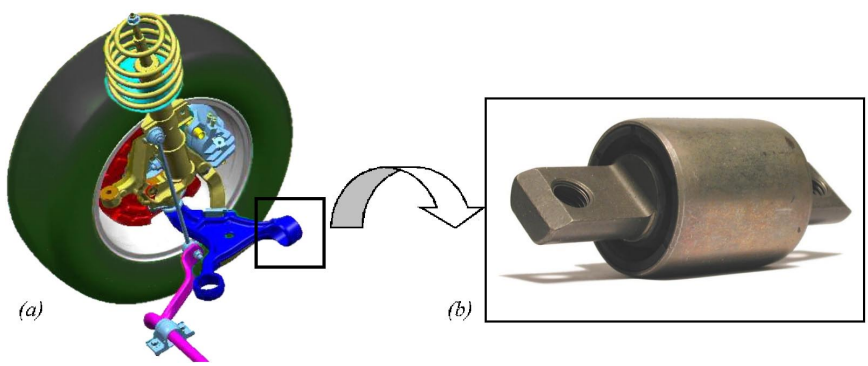

Figure 2.1: *(a) The position of the hydrobushing in the front wheel suspension. (b) The hydrobushing.*

Figure 2.1(b) shows a photo of the hydrobushing. It consists of natural rubber, chambers containing glycol, and a steel axle and cover. The glycol has a low freezing point, which enables the bushing to perform well under winter conditions. The glycol can stream between chambers through channels. The presence of the fluid gives the hydrobushing about ten times higher damping than a conventional rubber bushing. In Figure 2.2 the interior of the hydrobushing can be seen. The cover has been removed and the chambers are exposed.

The hydrobushing can be designed to fulfil special requirements with respect to its damping properties, since the peak damping occurs at the resonance frequency of the fluid. By slightly varying the design of the chambers or channels, or the amount of fluid encapsulated, the resonance frequency can be changed. Two interesting damping applications are sudden bumps, i.e. large displacement amplitude and

Figure 2.2: *The hydrobushing parts. Interior and cover.*

low frequency, and engine vibrations, i.e. low amplitude and high frequency. The component studied in this Master's thesis is designed to give high damping for low amplitudes (typically 0.10-0.20 mm) at frequencies in the range of 15-20 Hz (wheel hop frequency).

The dynamic characteristics of the hydrobushing have very strong frequency dependence due to the fluid encapsulated. The amplitude and frequency dependence are *coupled* for a hydrobushing. This will be discussed more thoroughly in Chapter 3.

Chapter 3

Laboratory experiments

This chapter concerns testing of the Volvo hydrobushing. Static, quasi-static, and steady state harmonic dynamic tests have been performed. The test results are analysed and hysteresis loops are studied in detail. Frequency and amplitude dependence with respect to dynamic stiffness and phase angle are also studied. The test results used in this Master's thesis are the same as in [3]. The test method is consequently also the same and Section 3.1 has therefore been copied from [3].

3.1 Test method

The tests have been carried out by Lars Janerstål at Volvo Car Corporation. All tests have been performed with a *Schenck* static/dynamic tensile testing machine, see Figure 3.1. The machine has a load cell of ± 7 kN maximum capacity and is able to measure at a frequency interval of 0.1-1000 Hz. The used software is *TEST STAR II*. The accuracy measured at the latest calibration occasion is less than $\pm 0.1\%$ in the middle of the measuring interval, and up to at the most $\pm 0.5\%$ at the wings of the interval.

The hydrobushing is mechanically conditioned to avoid Mullins' effect[1], see Figure 3.2. It is important to perform this conditioning properly because the usefulness of the test data depends on how the mechanical conditioning has been performed. The method to condition the component used in this Master's thesis is the *one-level conditioning*. This one-level method uses only one level of stretch in the conditioning procedure, which has been set to 110% of the maximum level used in the testing. In order to avoid heat build-up in the component it is important not to cycle the component too long. The component is exposed to 3 cycles. A disadvantage of the one-level method, is that it tends to lower the stiffness of the vulcanizate too much in regions of small stretch values, according to [1]. The tests have been designed to preserve the conditioning during the testing. Consequently, the tests have been performed with the highest amplitude first and continued with decreasing amplitudes

[1]Mullins' effect is attributed to breaking of the cross-links between the filler and the elastomeric material, which results in decreasing stiffness for increasing strain amplitude

[3].

Figure 3.1: *The machine used for testing. A Schenck static/dynamic tensile testing machine [3].*

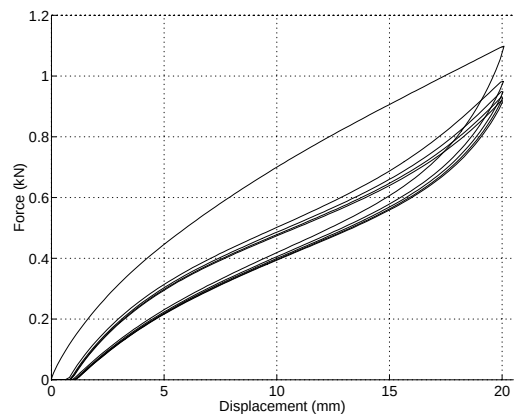

Figure 3.2: *The one-level conditioning of rubber components [3].*

3.2 Overview of performed tests

Static, quasi-static, and steady state harmonic dynamic tests of the component, have been performed by the Material Centre laboratory of Volvo Car Corporation. The hydrobushing has been tested in the radial direction. The tested amplitudes are listed in Table 3.1.

The static tests have been conducted with a triangular displacement history, i.e. with a constant velocity. The hydrobushing is tested with v=0.05 mm/s except for the amplitudes 0.5 mm, 0.2 mm, and 0.12 mm, which are tested with v=0.01 mm/s. The quasi-static tests have been performed with a sinusoidal displacement history at 0.03 Hz. The dynamic tests have been performed as discrete frequency sweeps (1-41 Hz, $\Delta f = 2$ Hz) for a given amplitude.

Tests	Amplitude [mm]
Static tests	*0.12, 0.20, 0.50, 0.80, 1.0, 1.5, 2.0, 3.0, 4.0, 4.5*
Quasi-static tests	*0.20, 0.50, 0.80, 1.0, 1.5, 2.0, 3.0*
Steady state harmonic dynamic tests	*0.10, 0.20, 0.50, 0.80, 1.0, 1.5, 2.0*

Table 3.1: *Performed tests.*

3.3 Analysis of experimental data

The experimental test results are presented and analysed in this section. The focus is on hysteresis loops, but frequency and amplitude dependence with respect to dynamic stiffness and phase angle are also studied. Non-linear elastic behaviour is expected for the hydrobushing when it is subjected to large displacements.

3.3.1 Static tests

Static test results are presented in Figure 3.3. The amplitude dependence for large displacements in Figure 3.3(a) and (b) is due to non-linear elasticity. Amplitude dependence caused by frictional damping can be seen in Figure 3.3(c) and (d), where increasing amplitude gives decreasing dynamic stiffness.

3.3.2 Quasi-static tests

Quasi-static test results are presented in Figure 3.4. The non-linearities for displacement amplitudes larger than 2.0 mm is due to non-linear elasticity, see Figure 3.4(a). Amplitude dependence caused by frictional damping can be observed in Figure 3.4(b).

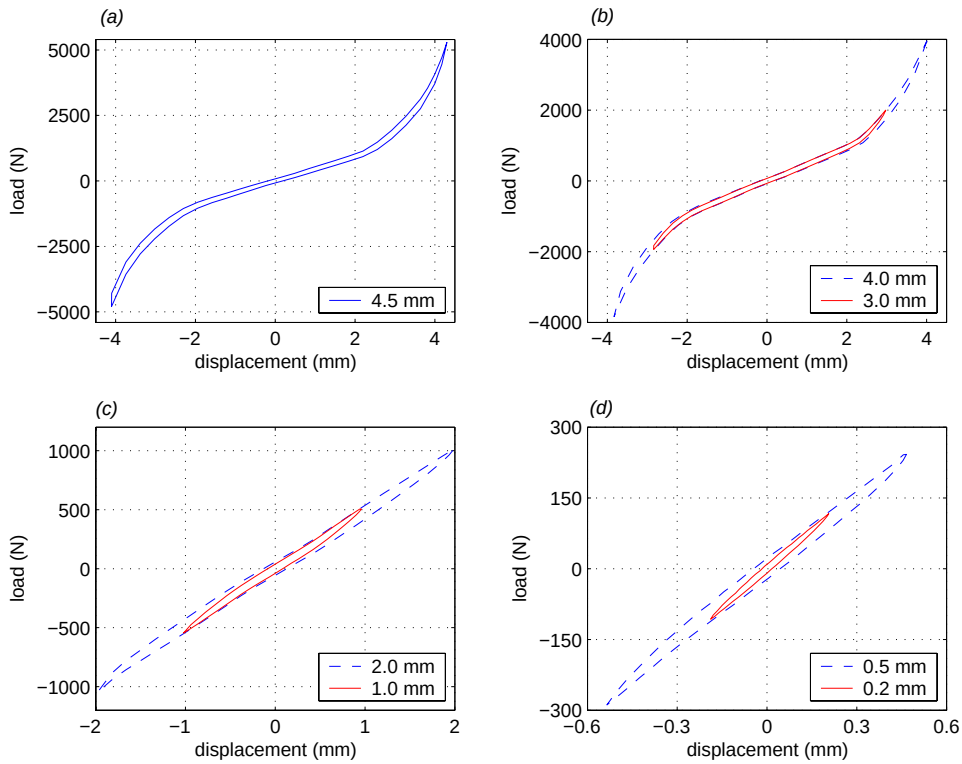

Figure 3.3: *Static characteristics for the hydrobushing.*

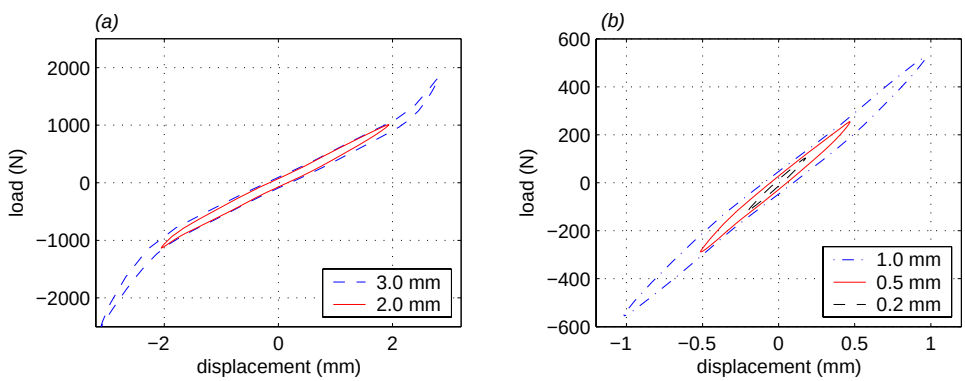

Figure 3.4: *Quasi-static characteristics for the hydrobushing.*

3.3.3 Dynamic tests

Steady state harmonic dynamic tests will be referred to as dynamic tests in the rest of this thesis. The dynamic test results are presented in Figure 3.5-3.8. Figure 3.5-3.7 are copied from [3].

Dynamic stiffness[2] and phase angle as function of amplitude and frequency are plotted in Figure 3.5. 2D representations of Figure3.5 is shown in Figure 3.6 and 3.7. The dynamic characteristics of the hydrobushing have a strong frequency dependence due to the fluid encapsulated.

The dynamic stiffness of the hydrobushing has a strong amplitude and frequency dependence for small amplitudes. This can be observed in Figure 3.5(a), 3.6(a), and 3.7(a). The phase angle is a measure of damping, i.e. a large phase angle indicates high damping. The hydrobushing is designed to give high damping at low amplitudes, 0.10-0.20 mm, and frequencies between 15-20 Hz (wheel hop frequency). This property is confirmed by Figure 3.5(b), 3.6(b), and 3.7(b). Conclusions drawn from Figure 3.5-3.7 are:

- the dynamic stiffness and phase angle have strong frequency dependence for small amplitudes
- the dynamic stiffness and phase angle have weak amplitude and frequency dependence for large amplitudes
- the hydrobushing has coupled amplitude and frequency dependence

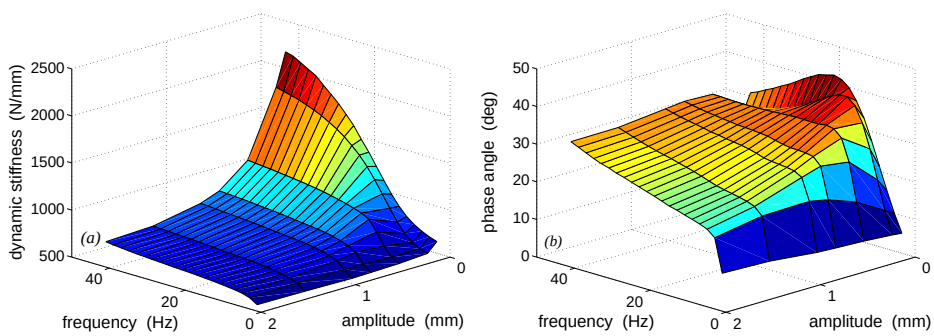

Figure 3.5: *Dynamic characteristics for the hydrobushing. Dynamic stiffness (a) and phase angle (b) as function of amplitude and frequency [3].*

[2]Dynamic stiffness is defined as $K_{dyn} = F_0/d_0$, where F_0 is the load amplitude and d_0 the displacement amplitude. The dynamic stiffness is a measure of the inclination of the hysteresis loop

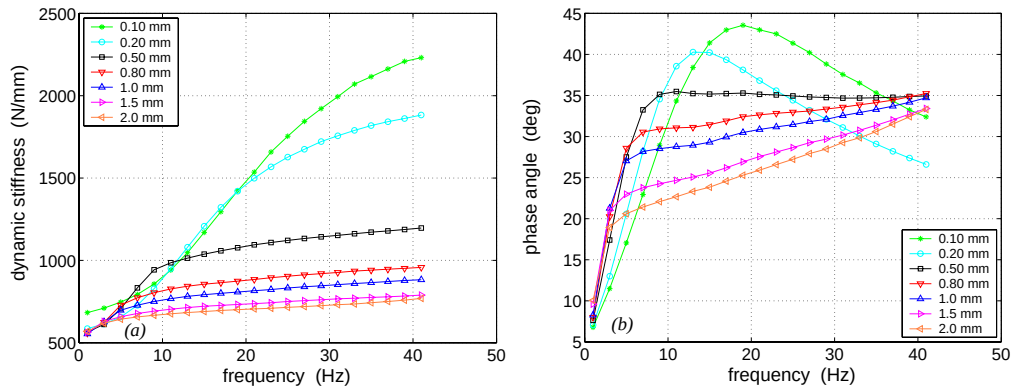

Figure 3.6: *Dynamic characteristics for the hydrobushing. Dynamic stiffness and phase angle as function of frequency for different amplitudes [3].*

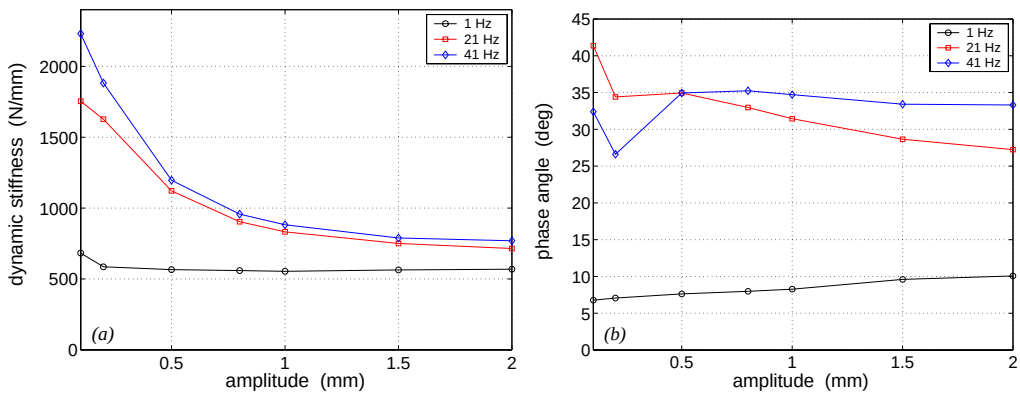

Figure 3.7: *Dynamic characteristics for the hydrobushing. Dynamic stiffness and phase angle as function of amplitude for some specific frequencies (1, 21, and 41 Hz) [3].*

The hysteresis loops for some different frequencies and amplitudes are presented in Figure 3.8. Three frequencies have been picked out for each displacement amplitude. These are presented in order to display the dynamic characteristics of the hydrobushing. The non-linearities for high frequencies are mainly due to viscous damping. The frequency dependence of the dynamic stiffness and phase angle is clearly seen for the small amplitudes, Figure 3.8(b)-(d). The frequency dependence is much weaker for larger amplitudes, see Figure 3.8(a).

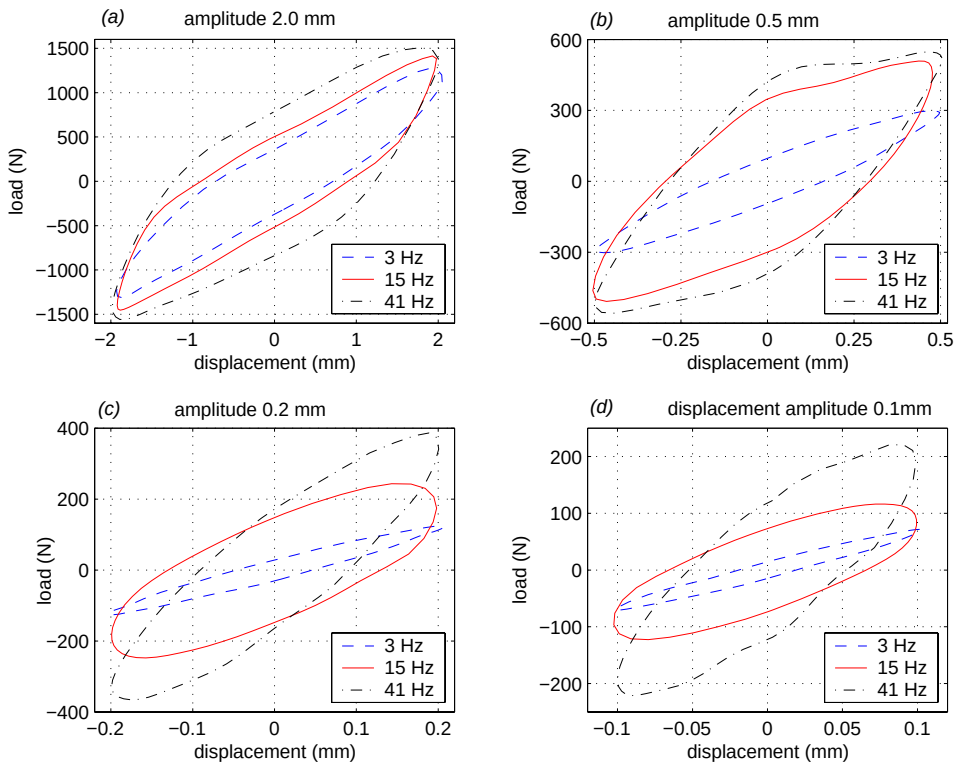

Figure 3.8: *Dynamic characteristics for the hydrobushing.*

Chapter 4

Hydrobushing modelling

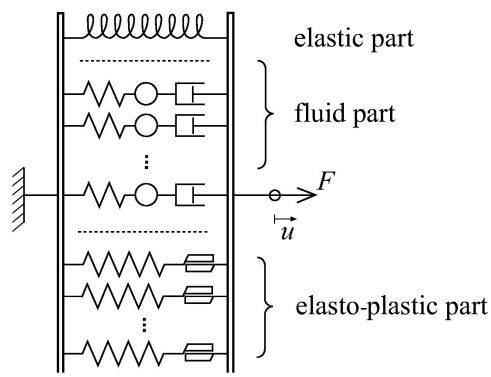

Figure 4.1: *One-dimensional model including elastic, fluid, and elasto-plastic properties.*

The hydrobushing has three kinds of damping - viscous, frictional, and fluid damping. One way to model the different kinds of damping is to combine one non-linear spring with several fluid and elasto-plastic elements in parallel according to Figure 4.1. This model is called the *hydrobushing model* and it will be shown that the model is able to fit static, quasi-static, and dynamic test results with reasonable accuracy. The stress expression is calculated by

$$\sigma = \sigma_e + \sigma_{fluid} + \sigma_{ep}$$

Several fluid and elasto-plastic elements make it possible to conduct a fit of the hysteresis loop to a wider frequency range and for larger variations in the amplitude.

The hydrobushing model is an expansion of the *generalized non-linear elastic viscoelastic elastoplastic model* used by Karlsson and Persson [3]. The difference between the two models is the fluid elements. The latter one has uncoupled amplitude and frequency dependence and is therefore not able to model the hydrobushing accurately. By substituting the visco-elastic elements for fluid elements, which represent

the enclosed glycol, the coupled amplitude and frequency dependent characteristics of the hydrobushing can be modelled.

4.1 Stress response algorithm

The algorithm for the stress contribution from the non-linear elastic and the elasto-plastic part of the model was derived in [3] and only the resulting expressions will be shown here. However, a thorough derivation of the stress contribution from the fluid part of the model will be presented in this section. The total load is a sum of the contributions from each element,

$$F_{total} = F_e + \sum_{i=1}^{nf} F^i_{fluid} + \sum_{i=1}^{np} F^i_{ep} \tag{4.1}$$

where nf is the number of fluid elements and np is the number of elasto-plastic elements.

4.1.1 Non-linear elastic part

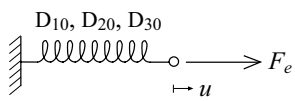

Figure 4.2: *The elastic part of the model represented by a non-linear spring.*

The non-linear model used to represent the elastic part is similar to the hyper-elastic constitutive Yeoh model in simple shear. This is a three-parameter model that only depends on the first strain invariant. The model has been proven to give a good fit to experiments carried out on filled rubbers [5]. The force-displacement relationship for the modified Yeoh model is

$$F_e = 2(D_{10}u + 2D_{20}u^3 + 3D_{30}u^5) \tag{4.2}$$

4.1.2 Fluid part

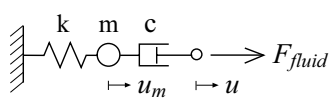

Figure 4.3: *The fluid element*

The fluid and viscous damping are modelled by the fluid elements. The fluid element consists of a linear elastic spring, a mass, and a dashpot connected in series,

according to Figure 4.3. Applying Newton's second law of motion on the mass gives

$$F_c - F_k = m\ddot{u}_m \tag{4.3}$$

where F_c and F_k are the forces in the dashpot and the spring respectively. The total force of the fluid element F_{fluid} is equal to the force in the dashpot

$$F_{fluid} = F_c = c(\dot{u} - \dot{u}_m) \tag{4.4}$$

and

$$F_k = ku_m \tag{4.5}$$

Combination of Equation (4.3)-(4.5) gives the equation of motion for the fluid element,

$$m\ddot{u}_m - c(\dot{u} - \dot{u}_m) + ku_m = 0 \Leftrightarrow m\ddot{u}_m + c\dot{u}_m + ku_m = c\dot{u} \tag{4.6}$$

Solving this second order differential equation gives the displacement of the mass, u_m, and the acceleration of the mass, $\ddot{u}_m$. Inserting the results into (4.3) gives the force contribution from one fluid element,

$$F_{fluid} = m\ddot{u}_m + ku_m \tag{4.7}$$

The second order differential equation is solved by using the MATLAB based CALFEM[1] function `step2`. This function computes, at equal time steps, the dynamic solution to a set of second order differential equations of the form

$$\begin{aligned} \mathbf{M}\ddot{\mathbf{u}} + \mathbf{C}\dot{\mathbf{u}} + \mathbf{K}\mathbf{u} &= \mathbf{f}(x,t) \\ \mathbf{u}(0) &= \mathbf{u}_0 \\ \dot{\mathbf{u}}(0) &= \mathbf{v}_0 \end{aligned}$$

$\mathbf{M}$,$\mathbf{C}$, and $\mathbf{K}$ represent the $n \times n$ mass, damping, and stiffness matrices respectively. The initial conditions are given by the vectors $\mathbf{u}_0$ and $\mathbf{v}_0$, containing initial displacements and velocities. Time integration constants for the Newmark family should be specified. Linear acceleration is used, giving $\alpha = \frac{1}{6}$ and $\delta = \frac{1}{2}$ [2].

Since the experimental series of data does not have equal time steps throughout one series, linear interpolation of the time vector is made. For each time step, a time vector with N minor time steps is created.

$$\mathbf{t} = [t_1 = t_i \quad t_2 \quad \dots \quad t_N \quad t_{N+1} = t_{i+1}]$$

In order to make the displacement vector correspond to the new longer time vector, cubic spline interpolation of the displacement vector is made. The `step2` function is then applied to these new displacement and time histories. The elements on the position $N+1$ in the result vectors, $\ddot{\mathbf{u}}$, $\dot{\mathbf{u}}$, and $\mathbf{u}$, are the acceleration, velocity, and displacement for the next original time step $i+1$. These results are used in (4.7) to calculate the next fluid load step, F^{i+1}_{fluid}.

In the MATLAB function for calculation of the fluid force the parameters are termed $m = M$, $k = K_f$, and $c = K_f \cdot Tr_f$, where Tr_f is the relaxation time for the dashpot, see Figure 4.4.

[1] CALFEM is a finite element toolbox to MATLAB. It is an interactive computer program for teaching the finite element method. The program can be used for different types of structural mechanics problems and field problems [2].

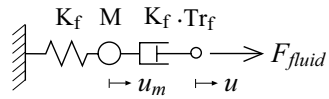

Figure 4.4: *The fluid element with model parameters.*

4.1.3 Elasto-plastic part

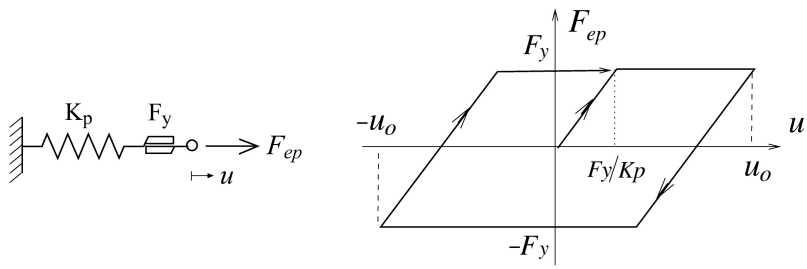

Figure 4.5: *(a) The elasto-plastic element. (b) The force-displacement relation for the elasto-plastic element.*

The frictional damping is symbolized by two blocks with sliding friction according to Figure 4.5(a). The friction is fully developed when the force in the element reaches the yield force, i.e. the model is elastic perfectly plastic and its force-displacement relation is shown in Figure 4.5(b). The algorithm used for determining the force contribution from one elasto-plastic element:

$$
\begin{aligned}
&i = 1, 2, 3... \\
&\quad \Delta u = u^{i+1} - u^i \\
&\quad F^{trial} = F^i + K_p \Delta u \\
&\quad \alpha = F_y / F^{trial} \\
&\quad if \;\; \alpha < 1 \;\; then \;\; \alpha = 1 \\
&\quad F^{i+1} = \alpha F^{trial}
\end{aligned}
$$

First the displacement increment Δu is calculated. Then the trial force, F^{trial}, is determined from the assumption that the response is purely elastic. F_y is the yield force. If the ratio $\alpha = F_y/F^{trial}$ is larger than 1 the frictional part of the element is sliding and the response of the element is no longer purely elastic. The next force level is then recalculated as αF^{trial}. If the ratio α is less than 1 the next force level is equal to the trial force.

Chapter 5

Fitting procedure

The goal of the fitting procedure is to determine the set of parameter values that gives the best fit of the model to experimental data. The fitting procedure is based on hysteresis loop fitting.

5.1 Error estimation

In order to find the set of parameter values that gives the best fit of the modelled displacement-load response to corresponding experimental data, each experimental data point is compared to the corresponding calculated one. The hydrobushing model is a displacement controlled model, i.e. the load is calculated from a known displacement history. Therefore the error is estimated as the difference between the calculated load value and the experimental load value for each data point. Since the load level will differ considerably from small displacement amplitudes to larger ones, also the size of the error will differ considerably and a relative measure of the error is desirable. This is achieved by dividing the absolute error by the load amplitude for the data series analysed. The error function resulting from this discussion, for each data point, is

$$\phi_i = \frac{|F_x^i - F_m^i|}{max|F_x|} \tag{5.1}$$

where the indices m and x stands for modelled and experimental, respectively. One series of data contains 53 data points, which describe one hysteresis loop for a certain displacement amplitude and frequency. A total of 92 series of data are used in the fitting procedure, of which 7 series are static, 5 are quasi-static, and 80 are dynamic.

In order to get an error estimation for the total fitting procedure, including all the experimental data, the error must be summarized in some way. The method chosen is:

1. Calculate the error for every data point in one series of data using (5.1).
2. Take the average of the errors calculated in 1 to represent the error of the series of data considered.

3. Repeat the procedure of 1 and 2 for every series of data.

4. The error for every series of data has now been calculated. Take the average of these errors to represent the total error of the model.

5.2 Error minimization

The fitting procedure aims at finding a set of parameter values giving an error as small as possible. The MATLAB function `fmincon` is used to find the minimum of the error function. The `fmincon` function finds a constrained minimum of a function of several variables. It solves problems of the form:

find min $F(\mathbf{X})$ if

$$\left.\begin{array}{rcl} \mathbf{AX} & \leq & \mathbf{B} \\ \mathbf{A}_{eq}\mathbf{X} & = & \mathbf{B}_{eq} \end{array}\right\} \textit{linear constraints}$$

$$\left.\begin{array}{rcl} C(\mathbf{X}) & \leq & \mathbf{0} \\ C_{eq}(\mathbf{X}) & = & \mathbf{0} \end{array}\right\} \textit{nonlinear constraints}$$

$$\mathbf{LB} \leq \mathbf{X} \leq \mathbf{UB} \quad \textit{lower and upper limits}$$

The vector $\mathbf{X}$ contains the parameters of the hydrobushing model. Not all of the available constraints are used in this fitting procedure. $\mathbf{X}$ is subjected to the linear constraint $\mathbf{AX} \leq \mathbf{B}$ in order to sort the fluid and elasto-plastic elements and set upper limits for some of the parameters. The linear constraints used result in a sorting of the elements according to

$$\begin{array}{ccccccc} Tr_{f_1} & \geq & Tr_{f_2} & \geq & \ldots & \geq & Tr_{f_{nf}} \\ F_{y_1} & \geq & F_{y_2} & \geq & \ldots & \geq & F_{y_{np}} \end{array}$$

Upper boundary vector, **UB**, and lower boundary vector, **LB**, are defined so that the solution $\mathbf{X}$ is found in the range $\mathbf{LB} \leq \mathbf{X} \leq \mathbf{UB}$. The boundaries are chosen on the basis of the initial values of the previously defined model parameters, the vector **Par0**, where

$$\mathbf{Par0} = [D_{10}, D_{20}, D_{30}, K_p^1 \ldots K_p^{np}, F_y^1 \ldots F_y^{np}, M^1 \ldots M^{nf}, K_f^1 \ldots K_f^{nf}, Tr_f^1 \ldots Tr_f^{nf}]$$

The lower limit is set to $0.1\mathbf{Par0}$ and the upper one to $10\mathbf{Par0}$.

5.3 Initial value estimation

The fitting procedure needs initial parameter values for the first error estimation. These initial values must be close enough to the best fit solution, otherwise the best fit will never be found. Estimations of the initial values are made using the experimental test results.

5.3.1 Elastic part

The elastic part of the model is represented by a non-linear elastic spring. The non-linear behaviour is described by the modified hyperelastic constitutive Yeoh model containing three parameters, D_{10}, D_{20}, and D_{30}. The initial values of these parameters are chosen to fit the hysteresis loop of the largest amplitude of the static tests [1]. This series of data is chosen because the non-linearities of the hysteresis loop is most evident for this series.

5.3.2 Elasto-plastic part

The elasto-plastic part of the model is represented by several elasto-plastic elements with two parameters, K_p and F_y, each. At low frequencies, the fluid contribution to the stiffness can be neglected and only the elastic and the elasto-plastic elements contribute to the stiffness [4]. The experimental data contains measurements of the dynamic stiffness for every series of data. If the fluid contribution can be neglected for frequencies ≤ 1 Hz, the dynamic stiffness at these low frequencies depends only on the elastic and the elasto-plastic parts of the model. For small amplitudes the non-linearities can be neglected and the stiffness of the elastic spring will be $2D_{10}$ according to Equation (4.2). The elasto-plastic contribution to the dynamic stiffness, K_p^{tot}, can then be estimated by

$$K_p^{tot} = K_{1Hz,0.1mm} - 2D_{10} \tag{5.2}$$

When the number of elasto-plastic elements is greater than one, and the stiffness of element i is K_p^i, K_p^{tot} according to (5.2) is considered to be the sum of all K_p^i. The initial distribution of the dynamic stiffness among the elasto-plastic elements is done according to

$$\begin{aligned} K_p^1 &= c \cdot K_p^{tot} \\ K_p^{i+1} &= (c-1)K_p^i, \qquad i = 2, \ldots, np-2 \\ K_p^{np} &= K_p^{tot} - \textstyle\sum_{i=1}^{np-1} K_p^i \end{aligned} \tag{5.3}$$

where the constant c is empirically set to 0.95 in order to obtain the parallelogram shape sought. This gives a distribution where the stiffness of element $i+1$ is 5% of the stiffness of element i.

The yield force F_y is the load level at which the frictional element starts to slide. Since frictional damping is not a prominent feature for small amplitudes, i.e. the area where the fluid damping is most evident (0.1-0.2 mm), the yield force can be estimated by

$$F_y^i = K_p^i(u_l + \Delta u(i-1)), \quad i = 1, 2, \ldots, np \tag{5.4}$$

where u_l is the lower displacement limit where frictional damping is introduced and Δu is the increase of this displacement limit for the next elasto-plastic element. u_l is

set to 0.2 mm and Δu is empirically chosen to be 0.1 mm. If $(u_l + \Delta u(i-1)) > 2.0$mm then the initial yield force will be estimated by

$$F_y^i = K_p^i \cdot 2.0mm \tag{5.5}$$

Equation (5.4) and (5.5) are valid for any number of elasto-plastic elements. If few elasto-plastic elements are used in the model, the frictional damping is introduced in the lower amplitude range, but if many elements are used the frictional damping will be introduced more even over the whole amplitude range. However, by experience, two elements are sufficient to get a satisfactory representation of the frictional damping.

5.3.3 Fluid part

The fluid part of the model is represented by several fluid elements with three parameters each; M, K_f, and Tr_f. The mass parameters are initially equally distributed and approximated in a way that the sum of them equals the weight of the encapsulated glycol,

$$M_i = \frac{M_{glycol}}{nf} \tag{5.6}$$

where nf is the number of fluid elements.

The dynamic stiffness at small amplitudes (0.1-0.2 mm), where the fluid part has greatest influence, is the sum of the stiffness contribution from each element in the model.

$$K_{tot} = 2D_{10} + K_p^{tot} + K_f^{tot} \tag{5.7}$$

where $K_f^{tot} = \sum_{i=1}^{nf} K_f^i$, and nf is the number of fluid elements. By assuming that the displacement amplitude is small, i.e. no frictional damping, and that the mass can be neglected, the model can be approximated by the standard linear solid model[1], see Figure 5.1, in order to determine the viscoelastic parameters of the fluid elements. The neglected mass is a rough approximation that will be corrected for later.

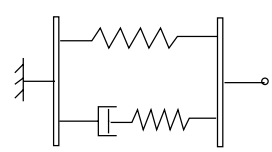

Figure 5.1: *The standard linear solid model.*

The relative amount of relaxation for the fluid elements g is set to 0.8. Figure 5.2 displays the definition of g in terms of normalized relaxation stiffness. By studying this figure an expression for g can be derived:

[1]The standard linear solid model is also known as the Zener model.

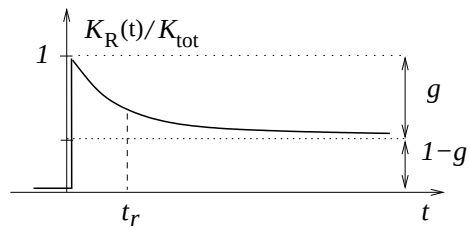

Figure 5.2: *The relative amount of relaxation, g, defined in terms of the normalized relaxation stiffness.* K_{tot} *is the instantaneous stiffness.*

$$\frac{K_R}{K_{tot}} \to 1 - g, \quad t \to \infty$$

$$K_R \to 2D_{10} + K_p^{tot}, \quad t \to \infty$$

$$1 - g = \frac{2D_{10} + K_p^{tot}}{K_{tot}} \quad \Rightarrow$$

$$g = \frac{K_f^{tot}}{K_{tot}} \tag{5.8}$$

The equation for the total stiffness contribution from the fluid elements is found by dividing (5.7) by K_{tot} and then using (5.8) and (5.7).

$$K_f^{tot} = \frac{g}{1-g}(2D_{10} + K_p^{tot}) \tag{5.9}$$

This total fluid stiffness is initially equally distributed amongst the fluid elements, i.e.

$$K_f^i = \frac{K_f^{tot}}{nf} \tag{5.10}$$

The relaxation time parameters distinguish one fluid element from an other. The relaxation time parameters are chosen to give high damping for frequencies between 10-20 Hz. The relation between frequency and relaxation time used is the relation valid for the standard linear solid model.

$$2\pi f \cdot Tr_f = 1 \Leftrightarrow Tr_f = \frac{1}{2\pi f} \tag{5.11}$$

The mass in the fluid element has great influence on the damping properties of the element. In the standard linear solid model all damping is due to the dash pot. Therefore (5.11) will be corrected with a factor in order to give reasonable

properties to the fluid element. The relaxation time parameter for each element is chosen in order to give peak damping at a frequency in the range f_{min}-f_{max}=10-20 Hz according to

$$\Delta f = \frac{f_{max} - f_{min}}{nf - 1} \tag{5.12}$$

$$Tr_f^i = c_1 \frac{1}{2\pi(f_{min} + \Delta f(i-1))} \tag{5.13}$$

where $i = 1, \ldots, nf$ and c_1 is an empirical correction factor. This factor is set to 0.1 [1].

5.4 Weighting

There is a possibility to give data of certain interest a greater influence in the parameter fitting process. This results in a better hysteresis fitting in the area of interest at the expense of worse fitting in other areas. The series of data to be weighted are specified by setting an amplitude range and a frequency range for the area of interest. The error estimation in (5.1) is then multiplied with a weighting factor set empirically to 3 for the selected series of data, giving the errors of these series greater influence in the total error estimation. When weighting is used Equation (5.1) is reformulated as

$$\phi_i = weight \cdot \frac{|F_x^i - F_m^i|}{max|F_x|} \tag{5.14}$$

Chapter 6

Validation

The hydrobushing model is validated for static, quasi-static, and dynamic loading by comparison of the calculated hysteresis loops with the corresponding experimental test results. The model used in this validation consists of one non-linear spring, two elasto-plastic elements, and two fluid elements. It is possible to vary both the number of elasto-plastic elements and the number of fluid elements, but from experience this combination gives satisfactory accuracy.

6.1 Expectation on the validation

The hydrobushing has a coupled amplitude and frequency dependence. The hydrobushing model developed in this work is expected to capture such a behaviour. The frequency and amplitude range to which the model is fitted is large and the model is not likely to fit well in the whole range. If very good fitting in a small range is desired, this range can be given greater importance during the fitting procedure by weighting, see Section 5.4.

6.2 Validation results

Most of the validation results presented in this section are not weighted. If weighting is used it is clearly stated in the text. The effect of weighting is more thoroughly discussed in Appendix A, where two different weighting ranges have been evaluated - one with greater importance for the 0.1 and 0.2 mm displacement amplitudes and the other with greater importance for the 1.0 and 2.0 mm amplitudes. This results in a better hysteresis fitting in the area of interest at the expense of worse fitting in other areas.

6.2.1 Static tests

The hysteresis loops for the static tests are plotted in Figure 6.1 together with the results from calculations using the hydrobushing model. The non-linearities of

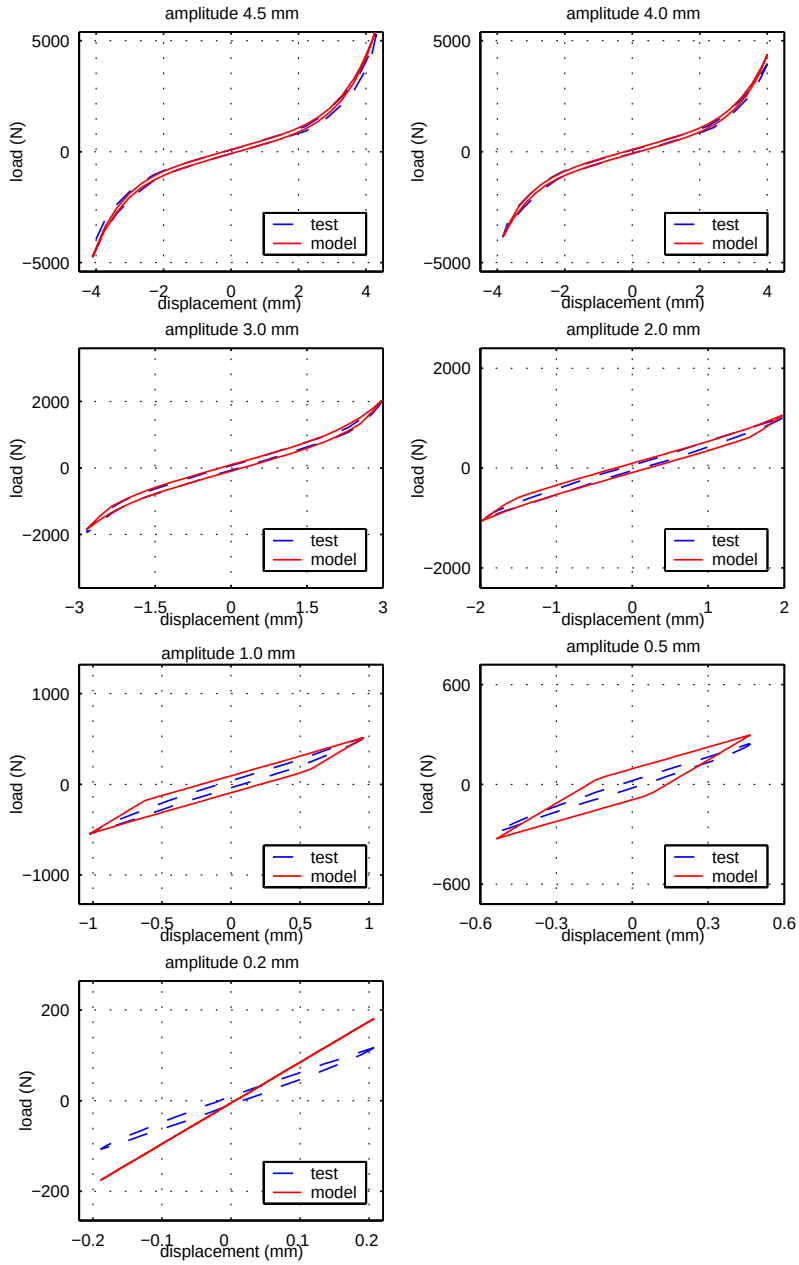

Figure 6.1: *Validation of the static series of data by comparison of experimental hysteresis loops (test) to calculated ones.*

the larger displacement amplitudes are modelled well. This was expected since the initial values of the non-linear parameters, the Yeoh parameters, were estimated in order to fit the largest static displacement amplitude. For displacement amplitudes smaller than 2.0 mm, the damping is overrated. The reason for the overestimation of the damping property is that the yield forces for the elasto-plastic elements are slightly too low, which will introduce frictional damping at too small displacement amplitudes. For the 0.2 mm displacement amplitude no frictional damping is active. This results in overestimation of the dynamic stiffness and underestimation of the damping (no damping present).

6.2.2 Quasi-static tests

The hysteresis loops for the quasi-static tests are plotted in Figure 6.2 together with the results from calculations using the hydrobushing model. The non-linearity of the largest quasi-static displacement amplitude is well captured by the hydrobushing model. The overestimation of the damping for displacement amplitudes smaller than 2.0 mm is due to frictional damping, see discussion in Section 6.2.1.

6.2.3 Dynamic tests

The hysteresis loops for some of the dynamic tests are plotted in Figure 6.3 and 6.4 together with the results from calculations using the hydrobushing model. The hysteresis loops for four frequencies - 3, 15, 21, and 41Hz - are presented for four different displacement amplitudes - 0.1, 0.2, 0.5, and 2.0 mm. These 16 hysteresis loops can be assumed to represent the frequency and displacement range evaluated, see Section 3.2 for more information on performed tests.

In Figure 6.3 the hydrobushing model seems to underestimate the damping for the 0.1 and 0.2 mm displacements. This is the case if no weighting is used. In Figure 6.5 the 0.1 and 0.2 mm displacement amplitudes have been weighted with a factor of 3 according to Section 5.4. The calculated hysteresis loops then fit the test results more accurately. The dominating damping in this area is fluid damping. In the hydrobushing model this type of damping has too great influence on larger displacement amplitudes, compared to experimental test results, i.e. if fluid damping is fitted to the hydrobushing area the damping is overestimated for larger amplitudes, see Appendix A. The fluid elements do not only influence the damping properties but also the dynamic stiffness. In Figure 6.3 the dynamic stiffness of the calculated hysteresis loops correlate poorly to the experimental test results. In Figure 6.5 the calculated dynamic stiffness is seen to fit the test results much better.

Frictional damping is the dominating type of damping for larger amplitudes although the fluid damping is still present for higher frequencies. The parallelogram shape of the experimental hysteresis loops in Figure 6.4 is due to frictional damping. In the hydrobushing model fluid damping has too great influence on large displacement amplitudes as mentioned above. This results in too little influence from frictional damping in order not to overrate the total damping. Therefore the

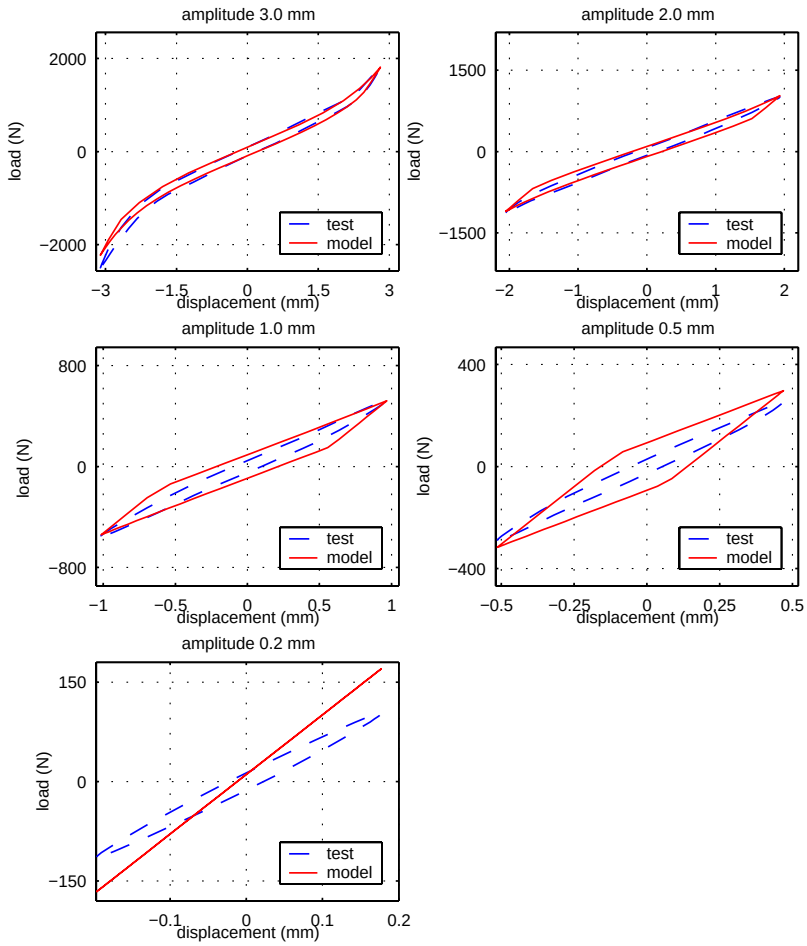

Figure 6.2: *Validation of the quasi-static series of data by comparison of experimental hysteresis loops (test) to calculated ones.*

parallelogram shape is not as prominent for the calculated hysteresis loops as for the test results. In order to get a better fit to large displacement amplitudes the 1.0 and 2.0 mm amplitudes are weighted with a factor of 3. The effect of this weighting on the displacement amplitudes 0.5 and 2.0 mm is presented in Figure 6.6. Weighting results in better fitting of the 2.0 mm amplitude. The fitting of the 0.5 mm displacement amplitude is seen to be worsen rather than improved. This is a result of the weighting that gives worse fitting in areas not weighted, and the 0.5 mm amplitude was not included in the weighting range.

6.2.4 Computation time

The fitting procedure is an iteration process, where the 13 model parameters are varied in order to minimize the deviation between the calculated response and experimental data. In every iteration step the elastic, elasto-plastic and fluid response are calculated for every data point in the hysteresis loops. The fluid response takes by far the longest time to calculate. In fact, it constitutes the great majority of the total computation time. The fluid response is computed using the CALFEM function `step2`, which computes the dynamic solution to the second order differential equation, Equation (4.6), at equal time steps. However, the time steps of the experimental data to which the calculated response should be compared are not of equal length, and therefore the time steps of the hydrobushing model cannot be of equal length either. The `step2` function must then be applied to every time step separately, giving an evident increase of the fitting time. The computation time of the total response is in direct proportion to the computation time of the fluid response.

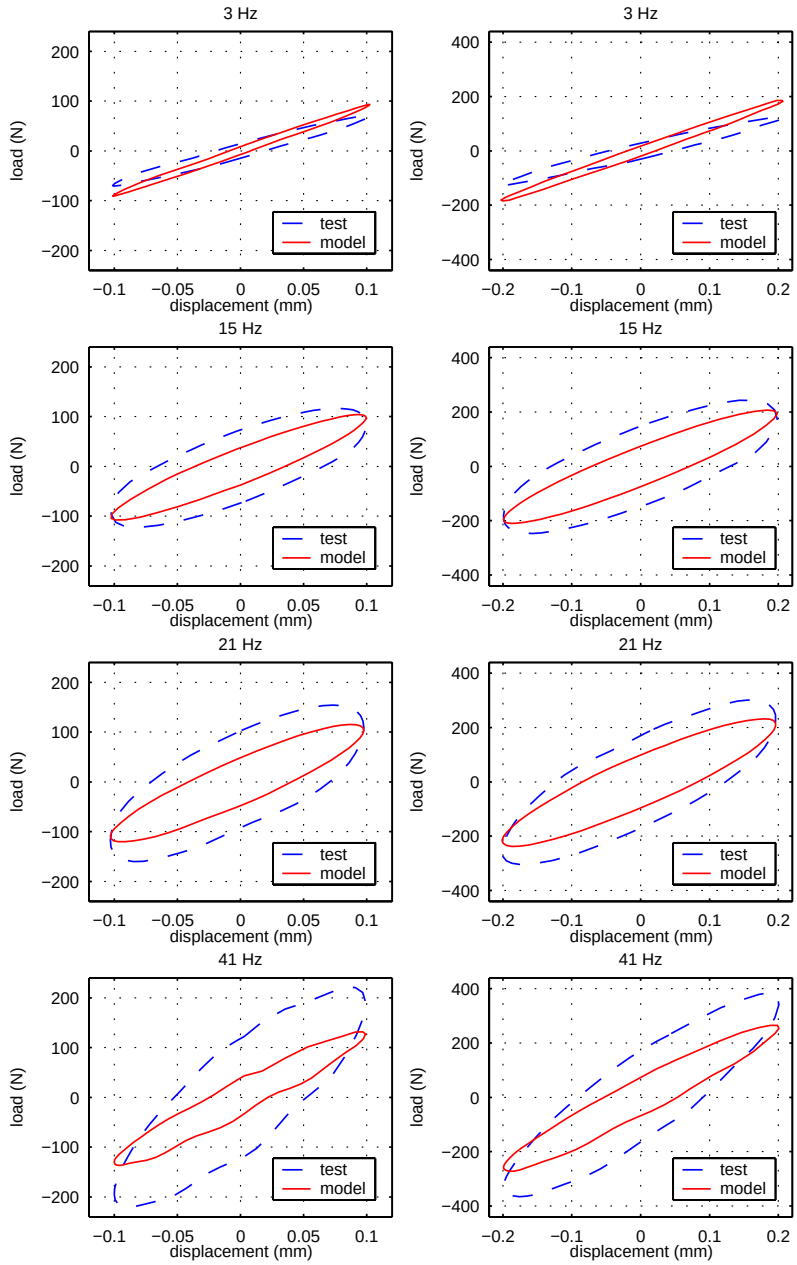

Figure 6.3: *Validation of the dynamic series of data by comparison of experimental hysteresis loops (test) to calculated ones (model). Displacement amplitudes 0.1 and 0.2 mm for some different frequencies.*

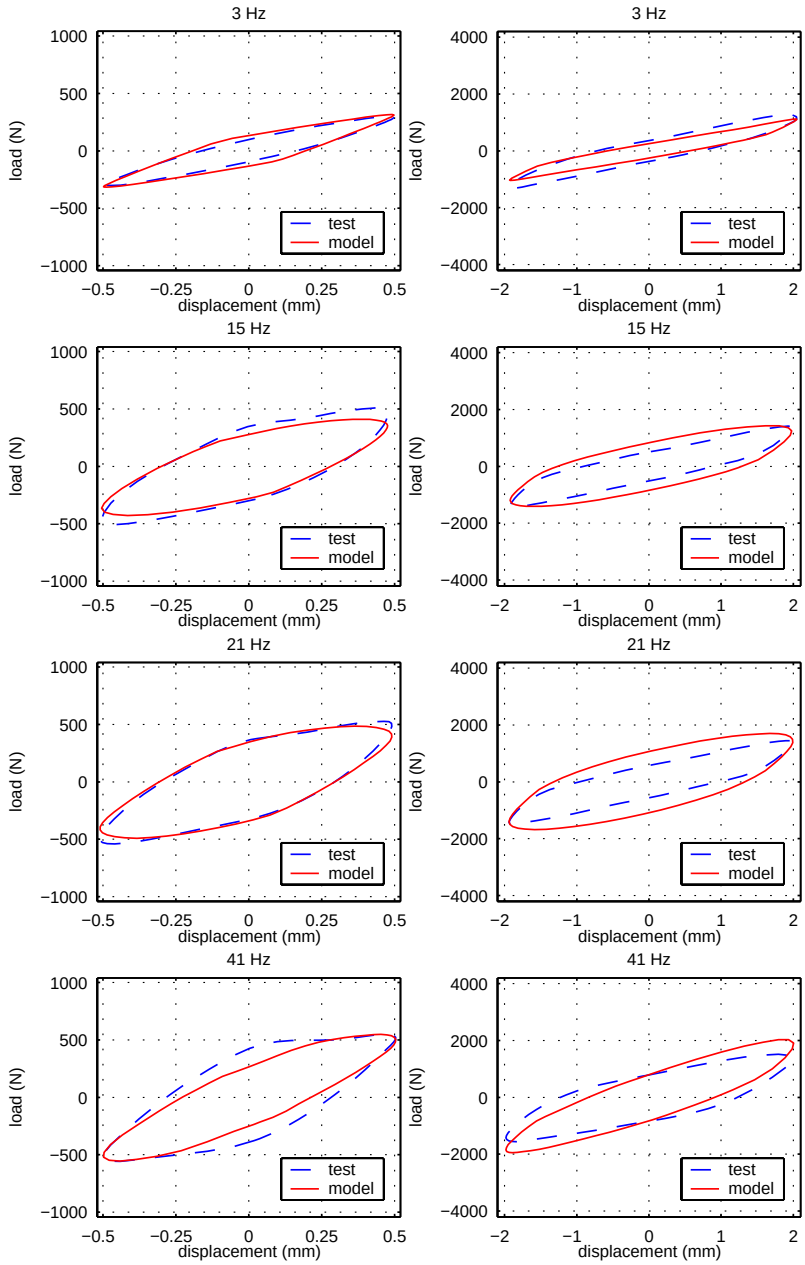

Figure 6.4: *Validation of the dynamic series of data by comparison of experimental hysteresis loops (test) calculated ones (model). Displacement amplitudes 0.5 and 2.0 mm for some different frequencies.*

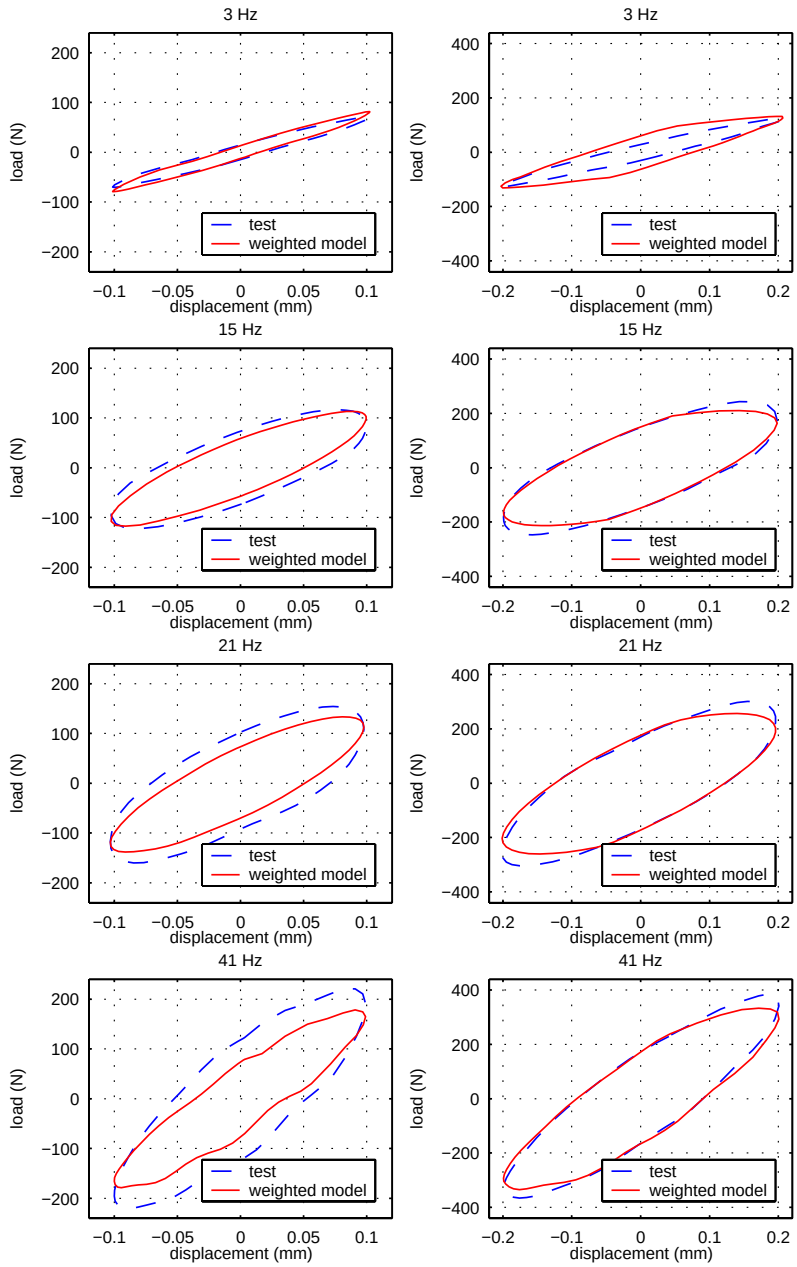

Figure 6.5: *Validation of the dynamic series of data by comparison of experimental hysteresis loops (test) to calculated ones (weighted model). Displacement amplitudes 0.1 and 0.2 mm for some different frequencies. Weighting of displacement amplitudes 0.1 and 0.2 mm with a factor of 3.*

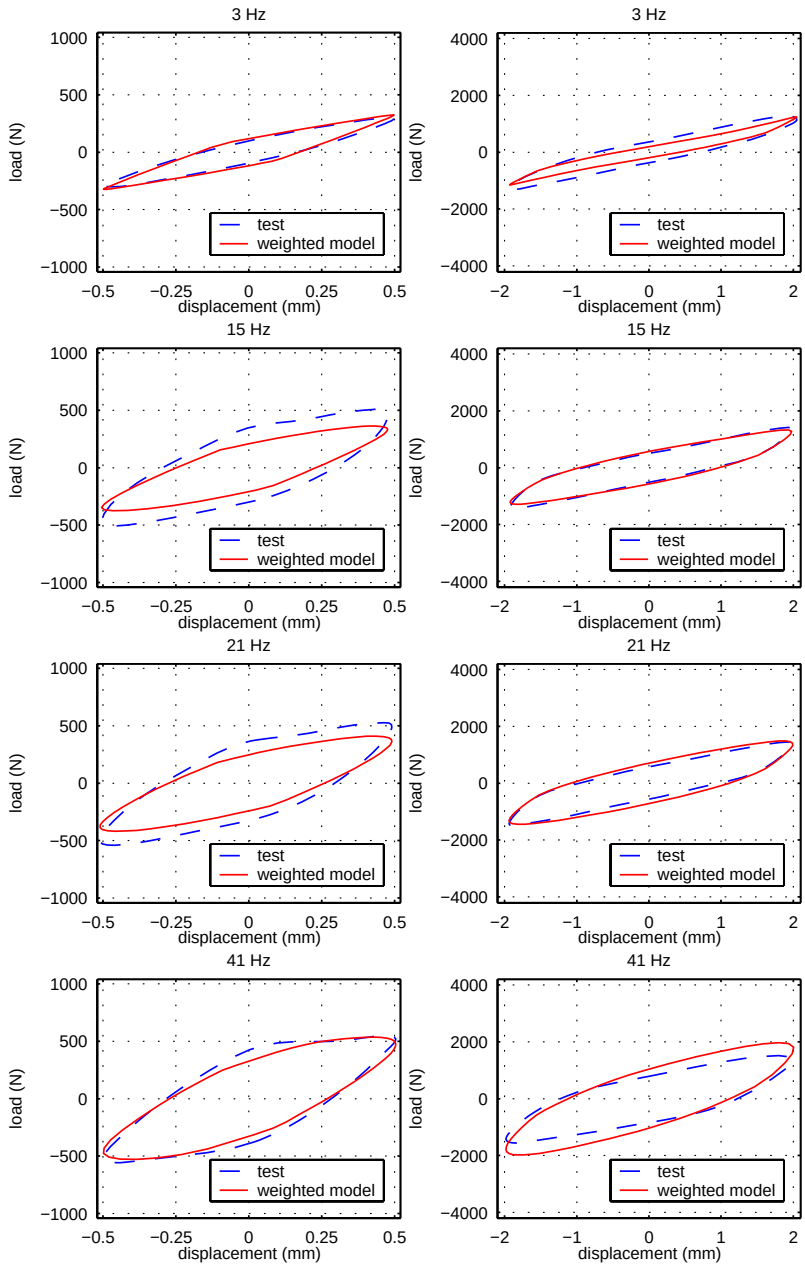

Figure 6.6: *Validation of the dynamic series of data by comparison of experimental hysteresis loops (test) to calculated ones (weighted model). Displacement amplitudes 0.5 and 2.0 mm for some different frequencies. Weighting of displacement amplitudes 1.0 and 2.0 mm with a factor of 3.*

Chapter 7

Summary and conclusions

The main objectives of this Master's thesis have been to establish a methodology for hydrobushing modelling and parameter identification. The major activities have been to:

- Propose a hydrobushing model, which models both rubber and fluid.
- Develop an automatized fitting procedure that fits the model parameters to the experimental results.
- Validate the hydrobushing model by comparison with component testing.

7.1 Hydrobushing model

The hydrobushing model proposed contains one elastic part, one elasto-plastic part, and one fluid part.

The elastic part consists of a non-linear spring, which can represent the non-linearities that arises at large displacement amplitudes.

The elasto-plastic part is composed of several elasto-plastic elements in parallel. Each element consists of a linear spring and a frictional element coupled in series. This part of the model captures the frictional damping of rubber.

The fluid part is composed of several fluid elements in parallel. Each element consists of a linear spring, a mass, and a linear dashpot coupled in series. This part of the model captures the viscous damping and the fluid damping peak for the resonance frequency of the fluid.

7.2 Fitting procedure

The hydrobushing model used in the validation part of this thesis consists of one non-linear spring, two elasto-plastic elements, and two fluid elements, giving 13 unknown

parameters. The values of these parameters were determined by an automatized fitting procedure that finds the set of parameter values giving the best fit of the model to experimental data. The steps in developing this procedure have been:

Error estimation. The fitting procedure is based on hysteresis fitting, i.e. each data point in the modelled hysteresis loop has been compared to the corresponding experimental test value. Summation of all data points gives the total error.

Error minimization. The MATLAB function `fmincon` was used to find the minimum of the total error. This function finds a constrained minimum of a function of several variables.

Initial value estimation. The fitting procedure needs initial parameter values in order to make the first error estimation. Estimations of the initial values were made using the experimental test results.

Weighting. The fitting procedure includes a possibility to give data of certain interest greater influence in the fitting process. This gives better hysteresis fitting in the range of interest at the expense of worse fitting in other ranges.

7.3 Validation

The hydrobushing model has been validated for static, quasi-static, and dynamic displacement controlled loading by comparison of the calculated hysteresis loops to the corresponding experimental ones. The model was expected to capture the coupled amplitude and frequency dependence of the hydrobushing.

Some observations from the validations:

- The non-linearities of the static and quasi-static loading at larger displacement amplitudes were modelled well.
- At static and quasi-static loading, the damping for displacement amplitudes smaller than 2.0 mm was overestimated due to the fact that frictional damping was introduced by the model at too small amplitudes.
- For dynamic loading the damping was underestimated for small displacement amplitudes. The dominating damping in this range is fluid damping. In the hydrobushing model this type of damping has too great influence on larger displacement amplitudes, compared to experimental test results, i.e. if fluid damping was fitted to smaller displacement amplitudes the damping would be overestimated for larger amplitudes.
- The parallelogram shape of the hysteresis loops for larger dynamic displacement amplitudes is due to frictional damping. In the hydrobushing model fluid damping has too great influence on large displacement amplitudes as

mentioned above. This results in too little influence from frictional damping in order not to overrate the total damping. Therefore the parallelogram shape is not as prominent for the calculated hysteresis loops as for the test results.

- By making use of weighting, much better fit in the weighted range was achieved.

For small amplitudes, 0.1 and 0.2 mm, the damping was underestimated for the whole frequency range, otherwise the damping follows its frequency dependence. For larger amplitudes, 1.0 and 2.0 mm, the damping property was correctly estimated for the lower frequencies, but overrated for the upper half of the frequency range, i.e. the damping did not follow its frequency dependence. Properties of the hydrobushing model:

The hydrobushing model:

- captures the behaviour of the static and quasi-static loading well.
- gives a satisfactory response for dynamic loading at amplitudes > 0.2 mm.
- does not represent the behaviour of dynamic loading at amplitudes ≤ 0.2 mm in a satisfying way.

7.4 Future work

Some suggestions for work within this field that can be done in the future:

- Develop a model that better captures the coupled amplitude and frequency dependence. A proposed model that may describe this behaviour more accurately is the model seen in Figure 7.1. This model has amplitude and frequency dependent elements coupled in series and is therefore expected to describe the coupled behaviour.

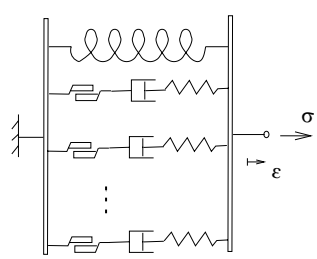

Figure 7.1: *Model with interrelated elastic, viscous, and frictional properties.*

- Shorten the computation time for the parameter fitting. By calculating the force contribution from the fluid elements analytically instead of using the numerical, time consuming CALFEM function `step2` the time needed to fit the model parameters to experimental data can be shorten.

- Extension of the 1D hydrobushing model to a 3D model. It is desirable to develop a hydrobushing model, which describes the behaviour of the component in 3D.
- Implementation of the hydrobushing model in MBS-codes such as ADAMS. This makes it possible to use the hydrobushing model in durability, handling, and ride comfort simulations.

Bibliography

[1] Austrell, Per-Erik. *Modeling of elasticity and damping for filled elastomers*, Report TVSM-1009, Lund University, Division of Structural Mechanics, Sweden, 1997, 58-64, 111-164.

[2] *CALFEM A finite element toolbox to MATLAB Version 3.3*, Report TVSM-99/9001, Lund University, Department of Mechanics and Materials, Division of Structural Mechanics and Division of Solid Mechanics, Sweden, 1999, 6.3 12-13.

[3] Karlsson, Fredrik and Anders Persson *MODELLING NON-LINEAR DYNAMICS OF RUBBER BUSHINGS - Parameter Identification and Validation*, Report TVSM-03/5119, Lund University, Division of Structural Mechanics, Sweden, 2003.

[4] Olsson, Anders K. *NON-LINEAR DYNAMIC PROPERTIES OF ELASTOMERS - Parameter Identification and Finite Element Analysis*, Report TVSM-03/3066, Lund University, Division of Structural Mechanics, Sweden, 2003, 49-72.

[5] Yeoh O.H. *Characterization of Elastic Properties of Carbon-black-filled Rubber Vulcanizates*, Rubber Chemistry and Technology, Vol. 63, pp. 792-805, 1990.

Appendix A

Validation of weighted fitting

The fitting procedure offers a possibility to weight an amplitude-frequency range of certain interest. This results in a better hysteresis fitting in the range of interest at the expense of worse fitting in other ranges. In this section, results from weighted fitting are presented and discussed.

A.1 Weighting of the fitting procedure

The series of data to be weighted are specified by setting a displacement amplitude range and a frequency range for the area of interest. In this range, the error for each data point is weighted with a factor of 3 according to

$$\phi_i = weight \cdot \frac{|F_x^i - F_m^i|}{max|F_x|} \tag{1.1}$$

where the indices m and x stands for modelled and experimental, respectively. The error contribution from the rest of the data is given by

$$\phi_i = \frac{|F_x^i - F_m^i|}{max|F_x|} \tag{1.2}$$

In order to get an error estimation for the total fitting procedure, including all the experimental data, the error must be summarized in some way. The method chosen is:

1. Calculate the error for every data point in one series of data using Equation (1.1) if the series will be weighted or else Equation (1.2).
2. Take the average of the errors calculated in 1 to represent the error of the series of data considered.
3. Repeat the procedure of 1 and 2 for every series of data.
4. The error for every series of data has now been calculated. Take the average of these errors to represent the total error of the model.

A.2 Validation of dynamic loading

Validation of two different weighting ranges have been carried out. The displacement amplitudes and frequencies that are weighted in the two fittings are:

- the *fluid* range - displacement amplitudes 0.1 and 0.2 mm for the whole frequency range.
- the *rubber* range - displacement amplitudes 1.0 and 2.0 mm for the whole frequency range.

The results of the validations are presented in Figure A.1 - A.4. In Figure A.1 and A.2 the fluid range has been weighted with a factor of 3 according to Equation (1.1). This procedure gives satisfactory fitting of the weighted displacement amplitudes, however, the farther away from the weighted range, the worse is the fitting. Similar conclusions is drawn when studying Figure A.3 and A.4. In the hydrobushing model fluid damping has too great influence on larger displacement amplitudes, and therefore the damping is greatly overestimated for large displacement amplitudes when fitting to the fluid range, see Figure A.2. In a similar way the damping is greatly underestimated for small displacement amplitudes when fitting to the rubber range, see Figure A.3.

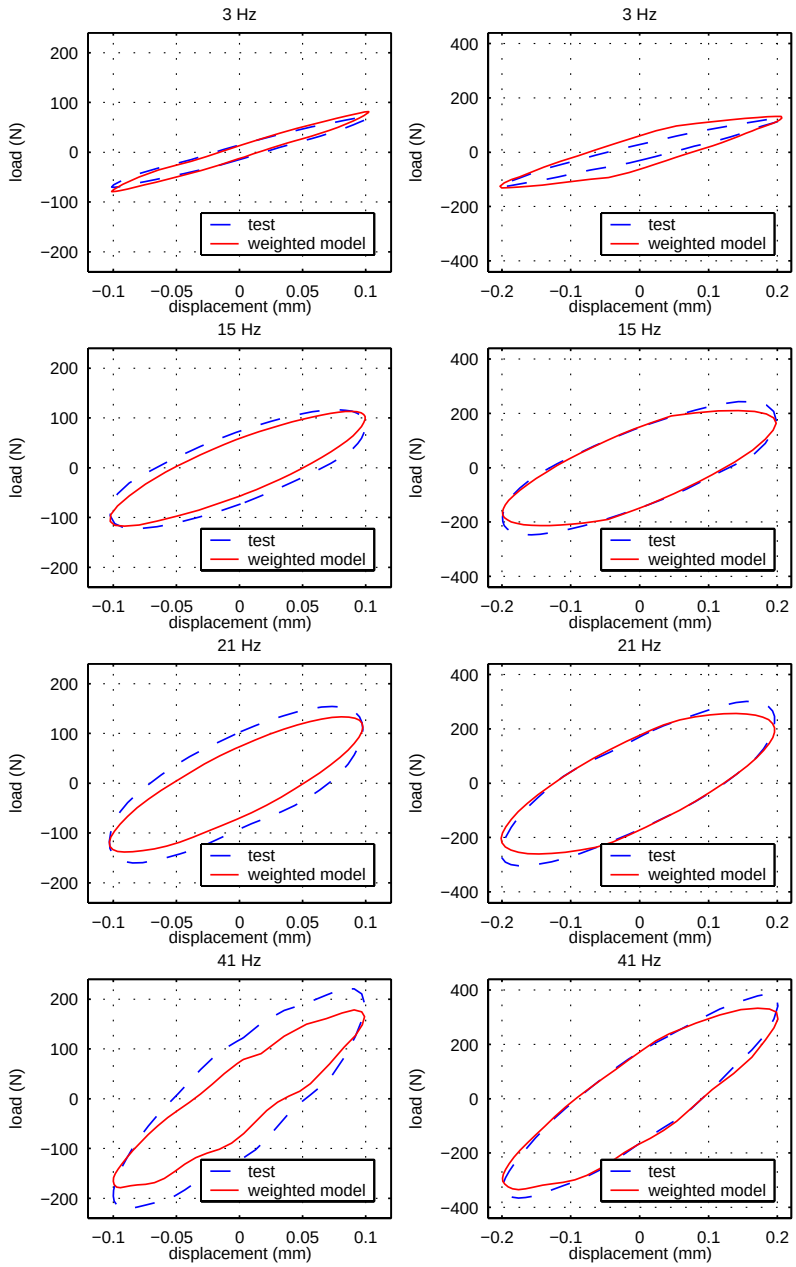

Figure A.1: *Validation of the dynamic series of data by comparison of experimental hysteresis loops (test) to calculated ones (weighted model). The* fluid *range has been weighted by a factor of 3. Displacement amplitudes 0.1 and 0.2 mm for some different frequencies.*

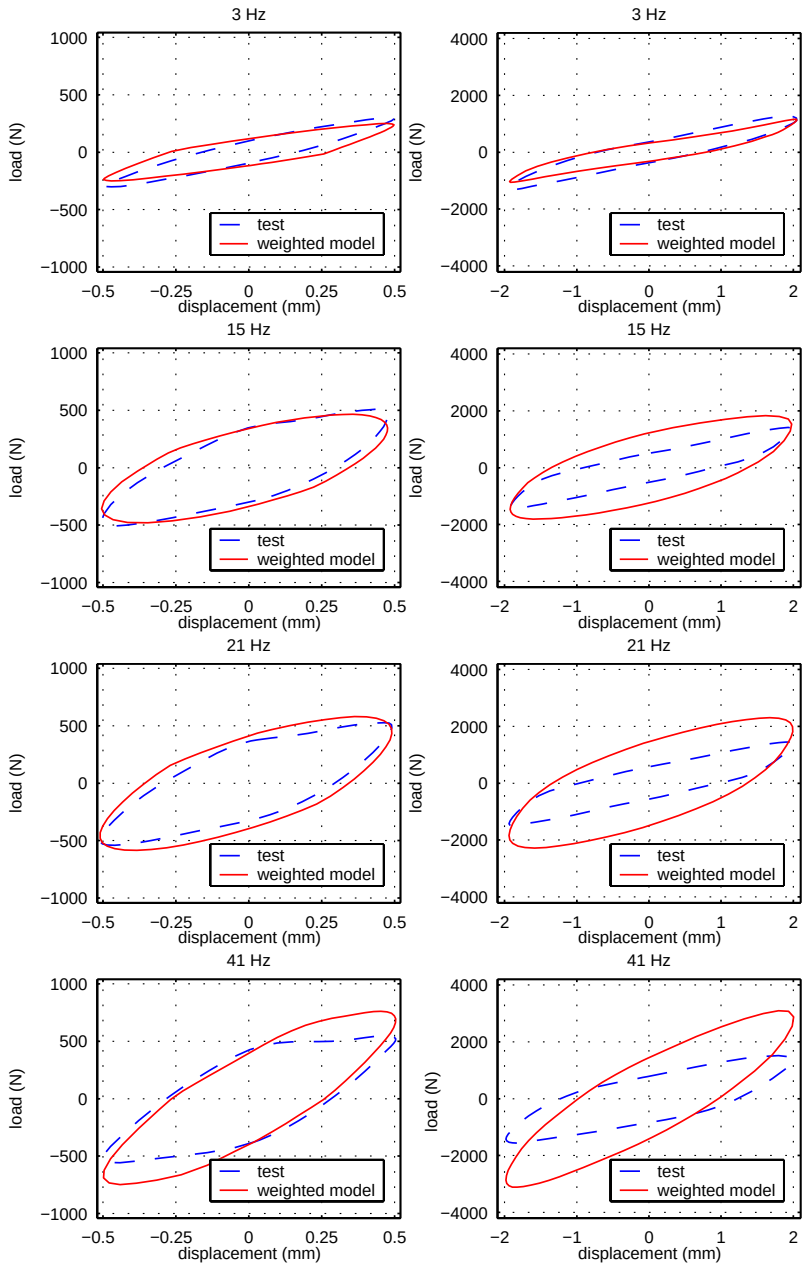

Figure A.2: *Validation of the dynamic series of data by comparison of experimental hysteresis loops (test) to calculated ones (weighted model). The* fluid *range has been weighted by a factor of 3. Displacement amplitudes 0.5 and 2.0 mm for some different frequencies.*

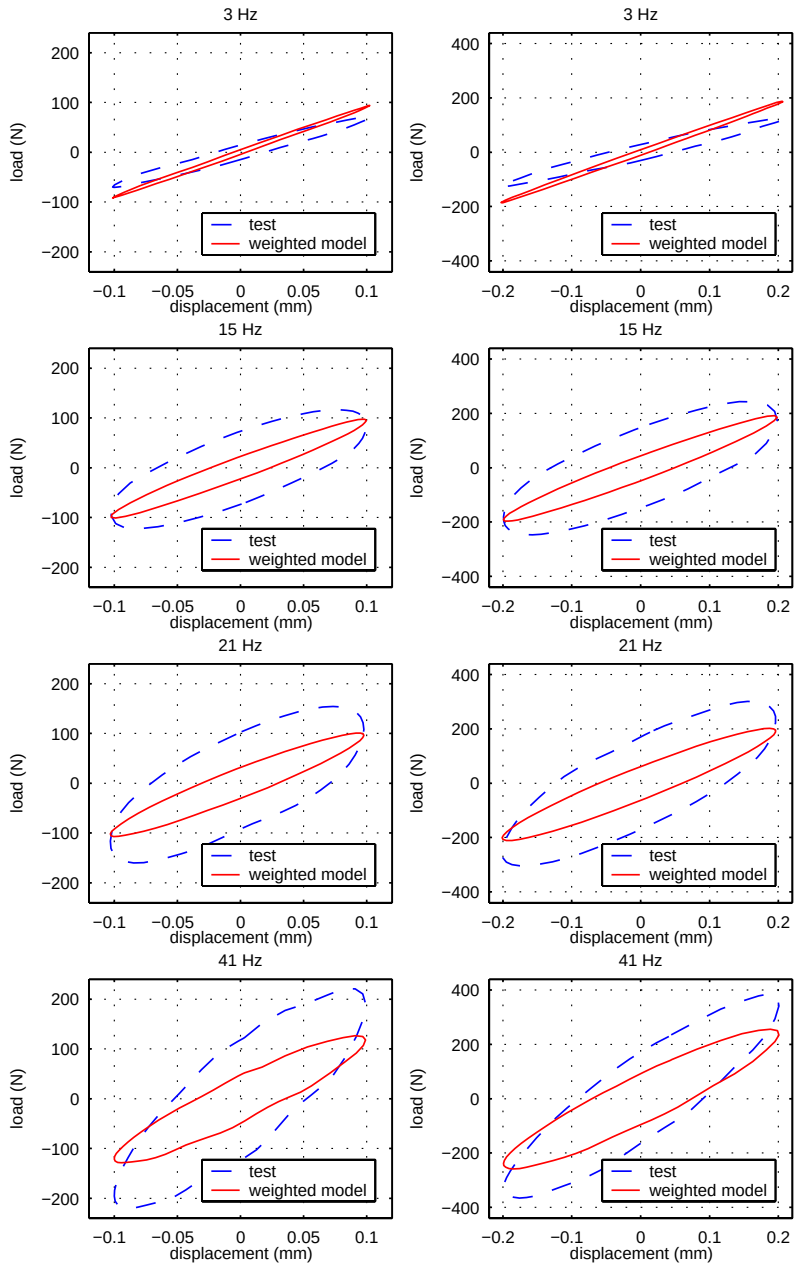

Figure A.3: *Validation of the dynamic series of data by comparison of experimental hysteresis loops (test) to calculated ones (weighted model). The* rubber *range has been weighted by a factor of 3. Displacement amplitudes 0.1 and 0.2 mm for some different frequencies.*

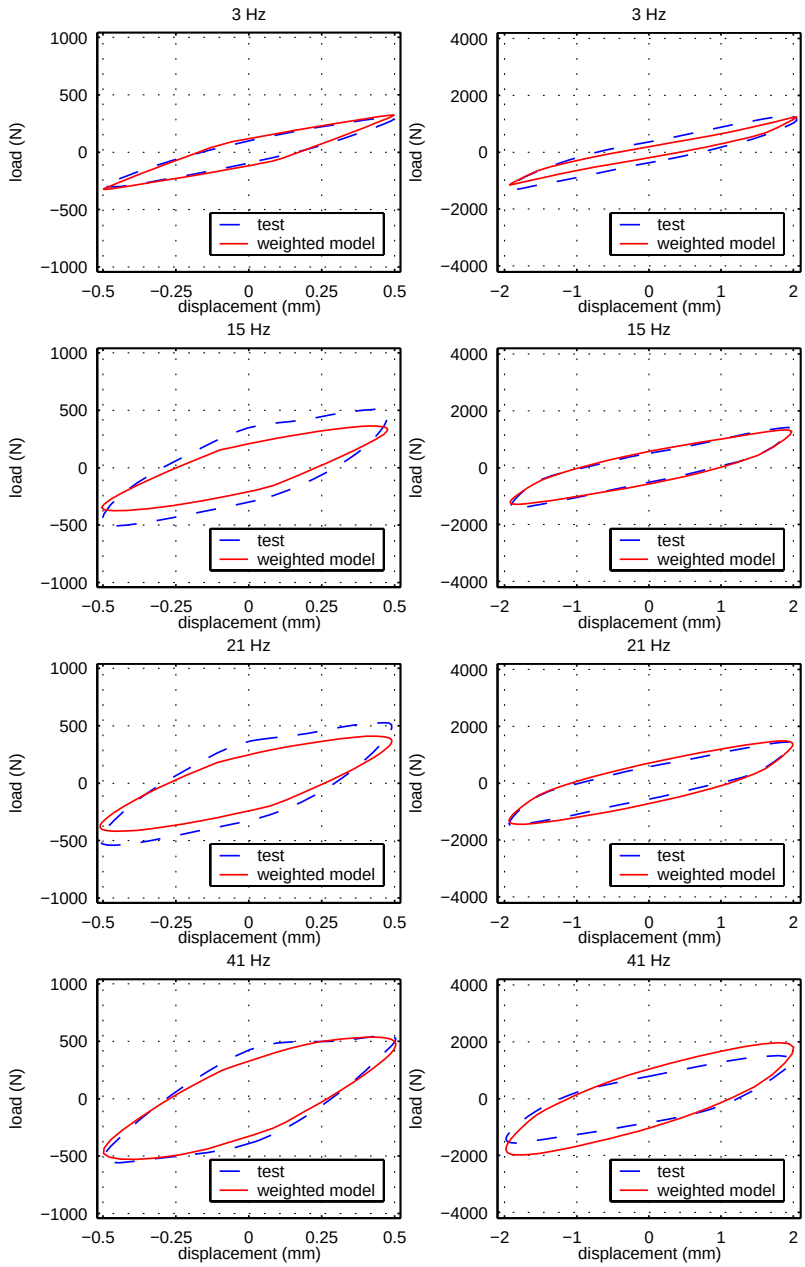

Figure A.4: *Validation of the dynamic series of data by comparison of experimental hysteresis loops (test) to calculated ones (weighted model). The* rubber *range has been weighted by a factor of 3. Displacement amplitudes 0.5 and 2.0 mm for some different frequencies.*

Appendix B

Parameter values

	no weighting	**0.1 and 0.2mm weighted**	**1.0 and 2.0mm weighted**
D_{10} (N/mm)	217.2	212.6	222.3
D_{20} (N/mm^3)	1.256	2.413	6.404
D_{30} (N/mm^5)	0.3461	0.2827	0.0265
K_p^1 (N/mm)	442.2	440.2	441.8
K_p^2 (N/mm)	23.27	21.39	22.70
F_y^1 (N)	88.44	84.37	89.79
F_y^2 (N)	4.652	0.04655	6.963
M^1 (kg)	0.01350	0.01413	0.004662
M^2 (kg)	0.001540	0.0001000	0.0001696
K_f^1 (N/mm)	1365.4	1365.5	1365.3
K_f^2 (N/mm)	1365.4	1365.5	1365.4
Tr_f^1 (s)	0.002602	0.002871	0.001842
Tr_f^2 (s)	0.0005057	0.002480	0.000007958
ϕ	0.1593	0.3881	0.2977
elapsed time (h)	2.26	5.30	6.49

Appendix C

MATLAB M-files

C.1 Main program

MAIN_ HYDRO.M

Purpose:

Determine the 1D hydrobushing model parameters.

Par = [D Kp Fy M Kf Trf]		1D hydrobushing model parameters
D	= [D10 D20 D30]	Yeoh parameters
Kp	= [Kp1 Kp2 ...]	spring stiffnesses (elasto-plastic part)
Fy	= [Fy1 Fy2 ...]	yield forces (frictional part)
M	= [M1 M2 ...]	fluid mass
Kf	= [Kf1 Kf2 ...]	spring stiffnesses (fluid part)
Trf	= [Trf1 Trf2 ...]	relaxation times (fluid part)

References:

Marie Håkansson and Malin Svensson 13-02-2004

Figure C.1 visualizes the program structure of the fitting procedure.

C.2 Routines used by the main program

C.2.1 LOAD_ INDATA.M and its subroutines

LOAD_ INDATA.M

Purpose:

Read dynamic, quasi static and static experimental data
and turn it into a proper format for further analysis.

References:

Marie Håkansson and Malin Svensson, 10-02-2004

Generated matrices:

DispX, LoadX, TimeX:
Each column of the matrices represents a time history
size (nbr timepoints) x (nbr series of data)

K, d0, f, dt:
Column vectors where each element correspond to a column
in the matrices DispX, LoadX and TimeX.

CORRECT.M

```
function[TimeX]=correct(DispX,TimeX,index_1)
```

Purpose:

Correct the time step at the start and the end
of the dynamic time history at the frequency 1 Hz.

References:

Marie Håkansson and Malin Svensson 19-12-2003

Input:

DispX, TimeX	experimental data
index_1	indices for the 1Hz series of data

Output:

TimeX	corrected time history

SINGLE_LOOP.M

```
function
[Disp,Load,Time,Disp_stat,Load_stat,Time_stat,Disp_quas,Load_quas,Time_quas]...
=single_loop(DispX,LoadX,TimeX,d0,index_1,DispX_stat,LoadX_stat,TimeX_stat,...
d0_stat,stl_stat,DispX_quas,LoadX_quas,TimeX_quas,d0_quas,stl_quas,index_fel)
```

Purpose:

Select one single hysteresis loop from the experimental data.
Every hysteresis loop contains the same nbr of data points.

References:

Marie Håkansson and Malin Svensson, 08-12-2003

Input:

DispX, LoadX, TimeX	experimental data
d0	displacement amplitude
index_1	indices for the 1Hz series of data
index_fel	indices for troublesome series of data
stl	sizes of the series of data (static and quasi static)

Output:

Disp, Load, Time experimental data (one period)

CENTER.M

```
function [Disp]=center(DispX,LoadX,f,dt)
```

Purpose:

Center the hysteresis loop with respect to the displacement.

References:

Marie Håkansson and Malin Svensson 02-12-2003

Input:

DispX,LoadX	experimental data
f	frequency
dt	time step

Output:

Disp	displacement (centered)

C.2.2 HYDRO_FIT.M and its subroutines

HYDRO_FIT.M

```
function [Par,phi]=hydro_fit(Par,DispX,LoadX,TimeX,f,np,nf,index_vikt)
```

Purpose:

Fit 1D hydrobushing model parameters to experimental load history.

References:

Marie Håkansson and Malin Svensson 13-02-2004

Input:

Par0 = [D Kp Fy M Kf Trf]	initial values
D = [D10 D20 D30]	Yeoh constants
Kp = [Kp1 Kp2 ...]	spring stiffnesses (elasto plastic part)
Fy = [Fy1 Fy2 ...]	yield forces
M = [M1 M2 ...]	fluid mass
Kf = [Kf1 Kf2 ...]	spring stiffnesses (fluid part)
Trf = [Trf1 Trf2 ...]	relaxation times
LoadX, DispX, TimeX	experimental data
f	frequency
np	nbr of elasto plastic elements
nf	nbr of fluid elements
index_vikt	indices for important series of data

Output:

Par	Fitted 1D hydro bushing model parameters
phi	relative error

ERROR_HYDRO.M

```
function [phi]=error_hydro(Par,DispX,LoadX,TimeX,f,np,nf,index_vikt)
```

Purpose:

Compute the relative error between experimental data
and calculated results in the 1D hydrobushing model

References:

Marie Håkansson and Malin Svensson 13-02-2004

Input:

Par = [D' Kp Fy M Kf Tr]	parameter values
D = [D10 D20 D30]	Yeoh parameters
Kp = [Kp1 Kp2 ...]	spring stiffnesses (elasto-plastic part)
Fy = [Fy1 Fy2 ...]	yield forces (frictional part)
M = [M1 M2 ...]	fluid mass
Kf = [Kf1 Kf2 ...]	spring stiffnesses (fluid part)
Trf = [Trf1 Trf2 ...]	relaxation times (fluid part)
DispX, LoadX, TimeX	experimental data
f	frequency
np	nbr of elasto-plastic elements
nf	nbr of fluid elements
index_vikt	indices for important series of data

Output:

phi	relative error

HYDROMODEL.M

```
function Load=hydromodel(Disp,Time,f,Par,np,nf)
```

Purpose:

Compute the load history for a given displacement history
using the 1D hydrobushing model

References:

Marie Håkansson and Malin Svensson 13-02-2004

Input:

Disp, Time	experimental data
f	frequency
Par = [D Kp Fy M Kf Trf]	parameter values
D = [D10 D20 D30]	Yeoh parameters
Kp = [Kp1 Kp2 ...]	spring stiffnesses (elasto-plastic part)
Fy = [Fy1 Fy2 ...]	yield forces
M = [M1 M2 ...]	fluid mass

Kf = [Kf1 Kf2 ...]	spring stiffnesses (fluid part)
Trf = [Trf1 Trf2 ...]	relaxation times
np	nbr of elasto-plastic elements
nf	nbr of fluid elements

Output:

Load	load history vector

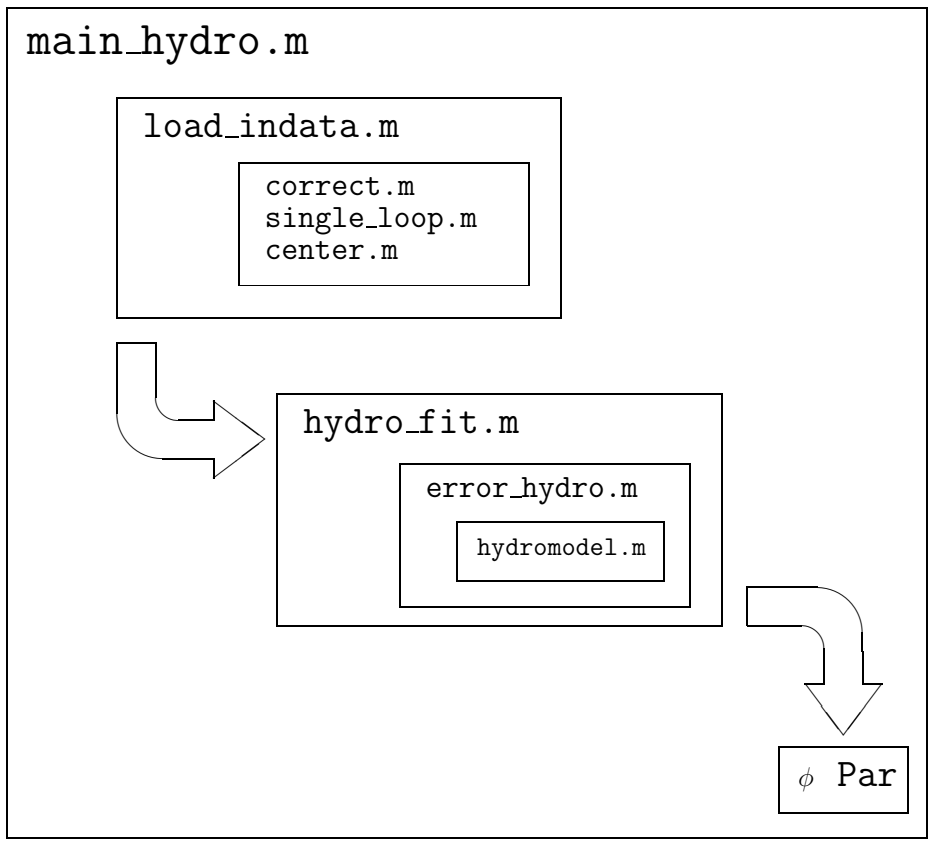

Figure C.1: *Description of the program structure.*